Video Article

A Mimic of the Tumor Microenvironment: A Simple Method for Generating Enriched Cell Populations and Investigating Intercellular Communication

Jason D. Domogauer[1], Sonia M. de Toledo[1], Edouard I. Azzam[1]

[1]Department of Radiology, New Jersey Medical School, Rutgers University

Correspondence to: Edouard I. Azzam at azzamei@njms.rutgers.edu

URL: https://www.jove.com/video/54429
DOI: doi:10.3791/54429

Keywords: Cancer Research, Issue 115, Cancer Biology, Tumor Microenvironment, Cancer-Associated Fibroblasts, Intercellular Communication, Gap Junctions, Extracellular Secretion, Permeable Microporous Membrane Insert, *In vitro* Culture Model, Hypoxia

Date Published: 9/20/2016

Citation: Domogauer, J.D., de Toledo, S.M., Azzam, E.I. A Mimic of the Tumor Microenvironment: A Simple Method for Generating Enriched Cell Populations and Investigating Intercellular Communication. *J. Vis. Exp.* (115), e54429, doi:10.3791/54429 (2016).

Abstract

Understanding the early heterotypic interactions between cancer cells and the surrounding non-cancerous stroma is important in elucidating the events leading to stromal activation and establishment of the tumor microenvironment (TME). Several *in vitro* and *in vivo* models of the TME have been developed; however, in general these models do not readily permit isolation of individual cell populations, under non-perturbing conditions, for further study. To circumvent this difficulty, we have employed an *in vitro* TME model using a cell growth substrate consisting of a permeable microporous membrane insert that permits simple generation of highly enriched cell populations grown intimately, yet separately, on either side of the insert's membrane for extended co-culture times. Through use of this model, we are capable of generating greatly enriched cancer-associated fibroblast (CAF) populations from normal diploid human fibroblasts following co-culture (120 hr) with highly metastatic human breast carcinoma cells, without the use of fluorescent tagging and/or cell sorting. Additionally, by modulating the pore-size of the insert, we can control for the mode of intercellular communication (*e.g.*, gap-junction communication, secreted factors) between the two heterotypic cell populations, which permits investigation of the mechanisms underlying the development of the TME, including the role of gap-junction permeability. This model serves as a valuable tool in enhancing our understanding of the initial events leading to cancer-stroma initiation, the early evolution of the TME, and the modulating effect of the stroma on the responses of cancer cells to therapeutic agents.

Video Link

The video component of this article can be found at https://www.jove.com/video/54429/

Introduction

The tumor microenvironment (TME) is a highly complex system comprised of carcinoma cells that co-exist and evolve alongside host stroma. This stromal component typically consists of fibroblasts, myofibroblasts, endothelial cells, various immune components, as well as an extracellular matrix[1]. A significant constituent, often the majority of this stroma, are activated fibroblasts, frequently referred to as cancer-associated fibroblasts or carcinoma-associated fibroblasts (CAF)[2,3]. Unlike normal, non-activated fibroblasts, CAFs contribute to tumor initiation, progression, angiogenesis, invasion, metastasis, and recurrence[4-11] in a wide variety of carcinomas, including breast, prostate, lung, pancreas, skin, colon, esophagus, and ovary[5,6,12-17]. Yet, the exact nature of the contribution of CAFs throughout cancer pathogenesis remains poorly defined. Furthermore, clinical evidence has demonstrated a prognostic value of CAFs, correlating their presence to high-grade malignancies, therapy failure, and overall poor prognosis[10,18,19].

Clearly, enhancing our understanding of the initiating events in CAF development, as well as the intercellular communications mediating their role within the TME, may provide exciting new therapeutic targets and enhanced strategies that could improve patient outcomes. Towards this goal, several *in vivo* and *in vitro* models have been developed. While *in vivo* approaches are more reflective of patients' TME, they possess limitations, including the immense complexity and heterogeneity both within and between tumors. Furthermore, tumor samples from human subjects often represent highly developed TME and do not permit an understanding of the TME initiating events. Experimental animal studies offer some advantages, however generalization of animal data to humans should be done with caution due to differences in physiology between humans and animals such as rodents (*e.g.,* thiol chemistry[20], metabolic rate[21], tolerance to stress[22], *etc.*). Further, unlike the human population, which is genetically heterogeneous in nature, laboratory animals are typically bred to homogeneity. Also, it is often difficult to examine transient physiological variations and cell phenotype changes, as well as to control for specific experimental parameters using animals such as rodents. Thus, *in vitro* 2- and 3-dimensional (2D and 3D) tissue culture models are frequently utilized to advance the basic understanding of TME development. In spite of their lack of an accurate portrayal of the complexity of *in vivo* systems, these models offer advantages that greatly facilitate mechanistic investigations. *In vitro* models allow for a more simplified, focused, and cost-effective analysis of the TME, whereby statistically significant data can be generated in cells free of systemic variations that arise in animals.

There are several varieties of *in vitro* systems. The two most commonly used TME *in vitro* models consist of mixed monolayer or spheroid cell cultures. Both culture methods are advantageous for basic studies of intercellular interactions (*e.g.,* normal cells with tumor cells) and for the analysis of various TME specific cell phenotype changes (*e.g.*, emergence of cancer-associated fibroblasts from normal fibroblasts). Additionally,

the spheroids are able to create a more reflective tissue-like structure of the TME, and can be representative of tumor heterogeneity[23]. However spheroids often produce widely varying oxygen tension gradients across layers, which may complicate experimental conclusions[24]. Unfortunately, both models are extremely limited in their ability to isolate pure cell populations for further characterization and study following co-culture. To do so would require at least one cell type to be fluorescently-tagged or labeled with an identifying maker, and then subjecting the mixed co-culture to extensive processing and cell sorting to separate the cell populations. While a cell sorter is capable of isolating a rather pure cell population, one must be cognizant of cellular stress and potential microbial contamination risks[25].

To facilitate the understanding of intercellular communication, great efforts have been devoted towards developing and optimizing *in vitro* systems that closely mimic the *in vivo* environment, while permitting a simplified approach. One such tool is the permeable microporous insert, a membrane substrate that was first developed in 1953[26] and subsequently adapted for diverse applications and studies (*e.g.*, cell polarity[27], endocytosis[28], drug transport[29], tissue modeling[30], fertilization[31], bystander effect[32,33], *etc.*). This system permits the growth of cells with *in vivo*-like anatomical and functional differentiation, as well as expression of many *in vivo* markers[34,35] that are not observed when cultured on impermeable plasticware. Furthermore, the extremely thin porous membrane (10 µm thick) permits rapid diffusion of molecules and equilibration times, which simulates the *in vivo* environment and permits independent cellular functioning at both the apical and basolateral cell domains. An additional advantage of the insert's utility as a TME system is its physical separation of two heterotypic cell populations grown on either side of the membrane in the same environmental conditions, while maintaining various modes of intercellular communication through the membrane pores. Though physically separated, the two cell populations are metabolically coupled via secreted elements and, as described here, also through gap-junctional channels. Additionally, by maintaining the inserts at *in vivo* partial oxygen tension (PO_2), the model reduces the complications of oxygen and chemical gradients observed in other systems. Rather, it increases the understanding of natural mechanisms controlling the TME. Notably, the two cell populations can be easily isolated with high purity, without fluorescent tagging and/or cell sorting following extended periods of co-culture.

Here we describe an *in vitro* TME protocol consisting of human breast carcinoma cells and human fibroblasts grown, respectively, on either side of a permeable microporous membrane insert, but yet in continuous bi-directional communication through the membrane pores. We show that by using membranes with different pore sizes, the contribution of a specific type of intercellular communication (*e.g.*, secreted factors versus gap junctions) to the development of the TME can be investigated.

Protocol

1. Preparation of Culture Media and Cells

1. Prepare 500 ml of Eagle's minimum essential medium supplemented with 12.5% (vol/vol) heat-inactivated fetal bovine serum (FBS), 2 mM L-alanyl-L-glutamine, and 100 units of penicillin and 100 µg of streptomycin per ml.
   NOTE: The growth medium and supplement(s) can be easily exchanged for the growth requirements of other cell strains or cell lines.
2. Prepare 70 µl of cell culture medium for each insert (6-well format insert): Eagle's minimum essential medium supplemented with 50% (vol/vol) heat-inactivated FBS, 2 mM L-alanyl-L-glutamine, and 100 units of penicillin and 100 µg of streptomycin per ml.
   NOTE: The medium is supplemented with 50% FBS to facilitate cell attachment to the bottom side (*i.e.,* underside) of the insert. The growth medium and supplement(s) can be easily exchanged for the growth requirements of other cell strains or cell lines.
3. Prepare a cell suspension of the cells destined to be plated on the bottom side of the insert.
   NOTE: Here, the results were obtained using AG1522 normal human fibroblasts grown in 75 cm^2 cell culture flasks, and these cells will therefore be the focus of description of the cell suspension's preparation.
4. To collect cells, remove the growth medium and wash the cell monolayer 2x with 5 ml 1x Phosphate Buffered Saline (PBS).
5. Remove the PBS and spread 1 ml of 0.25% (vol/vol) trypsin with 2.21 mM ethylenediaminetetraacetic acid (EDTA), pre-warmed to room temperature (RT) over the cells for 2 min at RT (room temperature).
6. Quench the trypsin activity with 9 ml of complete growth medium (prepared in step 1.1) and collect cells by gently pipetting the cell suspension over the surface of the flask 10x.
7. Determine the cell concentration by using a hemocytometer or electronic counter and pipette the cell suspension volume that will provide 250,000 cells per insert into a sterile 15 ml centrifuge tube.
8. Pellet the cell suspension by centrifugation (800 x g, 2 min). Suspend the cell pellet with growth medium (prepared in step 1.2) to create a concentration of 250,000 cells per 70 µl.
   NOTE: As cell culture in permeable microporous membrane inserts is based on 2D substrates, cell seeding is performed similarly, except the cells should be initially suspended in medium containing 50% (vol/vol) FBS to facilitate attachment.

2. Preparation of Inserts

NOTE: To ensure sterile conditions, work in a laminar flow biological safety cabinet dedicated to cell culture.

1. Select inserts with a membrane pore size of 0.4 µm, 1 µm, or 3 µm (determined by the experimental interest(s), as the pore size can be used to explore the role of different modes of intercellular communication).
   NOTE: The 0.4 µm pore is small enough to limit formation of functional gap junctions between cells on either side of the insert membrane and can be used to study intercellular communication by secreted factors. Whereas, the 1 µm and 3 µm pores are large enough to allow formation of functional gap junctions and can be used to study intercellular communication by both gap junctions and secreted factors.
2. Remove individual inserts from the packaging and place into an equally sized multi-well dish.
   NOTE: Inserts are available with various membrane surface areas to fit specific application needs (*e.g.*, 6-well, 12-well, and 24-well inserts). Here, the results were obtained using the 6-well insert, and will therefore be the focus of the model description.
3. Cover the dish, containing the inserts with the dish lid. Holding the multi-well dish with both hands, gently invert the dish such that the insert bottoms (*i.e.,* underside) are now facing upwards.

4. Remove the bottom of the multi-well dish, exposing the bottom side of the inserts. Working with one insert at a time, use a sterile pair of forceps and gently hold the insert in place. With the free hand, use a pipette with a wide-mouth tip to draw 70 µl of the cell suspension (prepared in steps 1.3-1.8), containing 250,000 cells.
5. To plate the cells, place the pipette tip gently on the center of the insert's membrane, and slowly pipette the 70 µl of cell suspension while slowly moving the pipette tip around the surface of the membrane. Be careful not to extend the pipette tip and cell suspension to the edge of the insert.
   NOTE: Touching the edge of the insert could result in loss of capillary tension of the cell suspension leading to the cells drying out during attachment.
6. Repeat for remaining inserts, with care being exercised not to work directly over the exposed inserts to avoid potential microbial contamination.
7. Gently return the multi-well dish bottom to cover the inserts. Keeping the dish with inserts inverted, incubate in a humidified air atmosphere of 5% (vol/vol) CO_2 at 37 °C for 30-45 min.
   NOTE: If the cell suspension on the insert contacts the bottom of the well, carefully lift the dish bottom and rest it on the edge of the dish top, so that it forms a slight angle and creates greater separation between the surface of the dish and the bottom side of the inserts (where the cells are seeded). This will prevent the cells from attaching to the surface of the wells instead of the insert.
8. Following the 30-45 min incubation time, gently remove the dish containing the inserts and place it in the laminar flow biological safety cabinet.
9. With two hands and keeping the dish lid tight, gently re-invert the dish such that the bottom side of the inserts containing the attached cells now faces down.
10. Slowly and carefully add 2 ml (1 ml for 3 µm pore inserts to avoid migration of cells through the insert pores) of pre-warmed complete medium (see step 1.1) to each well, so that the bottom of the insert is immersed.
11. After adding growth medium in all the wells containing inserts, place the dish back into the humidified incubator.
12. Allow the inserts to remain undisturbed in the incubator for 48 hr. After 48 hr, feed the cells by aspirating the 2 ml of medium from the bottom of the well and adding 2 ml of fresh growth medium.
13. After adding fresh medium to the bottom of the well, seed 1 ml of the second cell population suspension (~250,000 cells/ml) on the top side of the insert, which already has the first cell population growing on the bottom side (for these experiments, AG1522 (control) cells or cancer (experimental) cells are plated on the top of the inserts, which already have AG1522 cells, destined to become CAFs, growing on the bottom side of the inserts). Place the dish back into the humidified incubator.
    NOTE: If working with cells that do not adhere well to the bottom of the insert, these cells can be alternatively grown on the top side of the insert.
14. Change the medium at 24, 72, and 96 hr after seeding the second population of cells on the top side of the insert by aspirating the medium from the top of the insert and bottom of the well. Gently add 1 ml of fresh medium to the top side of the insert and 2 ml to the bottom of the well. Allow the two cell populations to remain in co-culture on either side of the permeable microporous insert membrane for 120 hr.

3. Collecting Cells from Insert by Trypsinization

NOTE: In addition to the ease of obtaining enriched cell populations, the insert TME model also allows for similar experimental treatments (*e.g.*, incubation with chemicals, exposure to oxygen conditions that are above or below ambient atmosphere, ionizing radiation treatment, *etc.*) as other *in vitro* TME co-culture models. Furthermore, the permeable insert co-culture substrate can be analyzed by procedures already developed for standard 2D tissue culture models. For example, cells can be harvested from either side of the insert membrane to obtain highly enriched populations, which can then be utilized for analysis of endpoints (*e.g., in situ* immuno-detection, Western blotting) or propagated for subsequent experiments[36].

1. To collect cells, remove the insert from the growth medium and place it into a 35 mm cell culture dish containing 1 ml PBS. Wash the bottom and top sides of the insert 1x with 1 ml PBS.
2. Remove the PBS and add 200 µl of 0.25% (vol/vol) trypsin with 2.21 mM EDTA, pre-warmed to RT.
    1. If collecting the cells grown on the bottom side of the insert, place the trypsin solution into the 35 mm dish and gently place the bottom of the insert into the trypsin solution for 2 min at RT.
    2. If collecting the cells grown on the top side of the insert, place the insert into a 35 mm dish and add the trypsin solution to the top of the insert and incubate for 2 min at RT.
3. Quench the trypsin activity by adding 800 µl of complete growth medium.
    1. If collecting the cells grown on the bottom of the insert, add the growth medium to the 35 mm dish and collect the cells by gently pipetting the 1 ml of cell suspension over the surface of the insert 10x, with the insert being held at a slight angle, such that the cell suspension collects into the dish.
    2. If collecting the cells from the top side of the insert, add the growth medium to the top side and gently pipette the 1 ml of cell suspension over the surface of the insert 10x.

4. Characterization of Cell Purity by Flow Cytometry

NOTE: To characterize the ability of the permeable microporous membrane inserts to maintain the purity of the two cell populations (*i.e.,* top and bottom) for up to 120 hr, sections 1-3 were performed, with green fluorescent protein (GFP)-tagged MDA-MB-231 cells being plated on the top side of the insert, and non-GFP-tagged AG1522 cells being plated on the bottom side of 0.4 µm-, 1 µm-, or 3 µm pore inserts.

1. Once the cells from the bottom side of the insert were collected (procedure described in Section 3), pellet the cell suspension by centrifugation (500 g, 30 sec).
2. Remove the supernatant and suspend the cell pellet in 400 µl of Hanks' Balanced Salt Solution (HBSS) supplemented with 1% (vol/vol) FBS.

3. Perform cytometric analysis on a flow cytometer equipped with a 488 nm laser to excite GFP and a bandpass filter of 530/30 to detect GFP photon emission[37].
4. For cell identification purposes, use AG1522 control cell populations to adjust forward and side scatter voltages on the flow cytometer. Adjust the GFP channel voltage to set the cellular autofluorescence value as the lower detection threshold for the GFP signal.
5. Determine gating threshold using control cells. Assess purity of each cell population based upon the presence of GFP-positive cells versus control.
   NOTE: A pure population would be reflective of no GPF-positive cells detected.

5. Characterization of Cells by *In Situ* Immunofluorescence

1. Following trypsinization of cells from the insert (see section 3), collect cells, plate 5 x 10^4 cells in 250 µl growth medium (see step 1.1) onto sterile glass coverslips, and allow to attach for 1 hr in a humidified air atmosphere of 5% (vol/vol) CO_2 at 37 °C incubator.
2. At the end of the incubation, gently remove the dish containing the coverslip and place it in the laminar flow biological safety cabinet.
3. Carefully add 2 ml of pre-warmed complete medium (see step 1.1) to each dish, so that the coverslip is immersed.
4. After adding growth medium to all the dishes containing coverslips, return the dishes to a humidified air atmosphere of 5% (vol/vol) CO_2 at 37 °C in an incubator for 48 hr.
5. Following the 48 hr incubation, wash the sample 3x with PBS and fix with 4% (wt/vol) formaldehyde in PBS for 10 min at RT.
6. Rinse 5x with Tris Buffered Saline (TBS: 50 mM Tris-Cl, pH 7.5, 150 mM NaCl) and then permeabilize with 0.25% (vol/vol) Triton X-100, 0.1% (wt/vol) saponin for 5 min at RT.
7. Block non-specific binding sites with 2% (vol/vol) normal goat serum (NGS), 1% (wt/vol) bovine serum albumin (BSA), 0.1% (vol/vol) Triton X-100 in TBS (blocking solution) for 1 hr at RT.
8. Incubate with primary antibody (anti-Caveolin 1 (CAV1), 1:1,000) in blocking solution at 4 °C overnight.
9. Wash off unbound primary antibodies (3x, 5 min/wash) with 0.2% NGS (vol/vol), 1% (wt/vol) BSA, 0.1% (vol/vol) Triton X-100 in TBS (wash solution).
10. Incubate with secondary antibody at RT for 1 hr in blocking solution (see section 5.4).
11. Wash off unbound secondary antibody (3x, 5 min/wash) with wash solution (see step 5.6).
12. Mount coverslips on a slide with an anti-fade mounting medium containing 4',6-diamidino-2-phenylindole (DAPI), and seal with nail polish.
13. Observe cells using a 63X oil magnification objective on an inverted microscope equipped with an external light source for fluorescence excitation, and capture images using an attached digital camera for subsequent analysis.

6. Characterization of Cells by Western Blot

NOTE: The Western blot procedure is described elsewhere[38]. A brief outline is described here:

1. Following detachment of cells from the insert by trypsinization (see section 3), pellet the cell suspension by centrifugation (500 g, 30 sec).
2. Remove supernatant and suspend the cell pellet 2x with 100 µl PBS.
3. Remove supernatant and lyse cells in 50 µl of modified radioimmunoprecipitation assay (RIPA) buffer (Tris pH 7.5 50 mM, NaCl 150 mM, NP40 1% (vol/vol), sodium deoxycholate monohydrate (DOC) 0.5% (vol/vol), sodium dodecyl sulfate (SDS) 0.1% (vol/vol)), containing protease and phosphatase inhibitor cocktail.
4. Incubate for 20 min on ice and centrifuge at 19,000 g for 15 min at 4 °C.
5. Determine concentration of proteins in the supernatant using a protein optical density assay, compatible with the detergents in the RIPA buffer.
6. Separate proteins by sodium dodecyl sulfate polyacrylamide gel electrophoresis (SDS-PAGE) and electroblot onto a 0.2 µm nitrocellulose membrane.
7. Incubate membranes in TBS containing 0.1% (vol/vol) Tween-20 (TBST) and 4% (wt/vol) skim milk (blocking solution) for 60 min and react with primary antibody at 4 °C overnight (anti-CAV1, 1:1,000).
8. Wash membrane 3x with TBST at RT (5 min/wash).
9. Incubate membranes for 30 min in blocking solution containing an anti-mouse secondary antibody conjugated with horseradish peroxidase (HRP) (1:5,000).
10. Wash membrane 3x with TBST at RT (5 min/wash).
11. Visualize reaction products by chemiluminescence using a Western blotting detection system.

7. Characterization of Intercellular Communication by Flow Cytometry

NOTE: To characterize the adaptability of the permeable microporous membrane inserts to examine different modes of intercellular communication (*e.g.,* secreted factors, gap junctions). Sections 1-2.12 were performed with non-fluorescent AG1522 cells being plated on the bottom side of 0.4 µm-, 1 µm-, or 3 µm-pore inserts.

1. Culture non-labeled AG1522 cells in a 35 mm dish to 90% confluency using medium described in section 1.1.
2. Rinse cells 1x with 1 ml of HBSS.
3. Load cells with Calcein AM by incubating cells in HBSS containing 30 µM of Calcein AM.
4. Incubate for 15 min in a humidified air atmosphere of 5% (vol/vol) CO_2 at 37 °C.
5. Wash cells 2x with 1 ml of HBSS.
6. Trypsinize cells by adding 200 µl solution of 0.25% (vol/vol) trypsin with 2.21 mM EDTA for 2 min at RT.
7. Quench the trypsin activity by adding 800 µl of complete medium containing 12.5% (vol/vol) FBS.
8. Bring cells into suspension by repeated pipetting.
9. Determine cell concentration by using a hemocytometer or electronic counter and plate 250,000 cells loaded with Calcein AM to the top side of inserts that already have AG1522 cells growing on the bottom side.

10. Incubate the inserts in a humidified air atmosphere of 5% CO_2 at 37 °C for 6 hr.
11. After 6 hr, collect cells from the bottom side of the inserts, as described in section 3.
12. Pellet the cell suspension by centrifugation (500 g, 30 sec).
13. Remove the supernatant and suspend the cell pellet in 400 µl of HBSS supplemented with 1% (vol/vol) FBS.
14. Analyze the cells on a cytometer equipped with a laser and filter capable of exciting and detecting the emission of Calcein (496 nm and 516 nm, respectively), per manufacturer protocol.
15. For cell identification purposes, use an unstained AG1522 control cell population to adjust forward and side scatter voltages on the flow cytometer. Adjust the Calcein channel voltage to set the cellular autofluorescence value as the lower detection threshold for the Calcein signal.
16. Determine the upper threshold limit using Calcein-loaded control cells. Assess communication for each cell insert based upon the presence of Calcein-positive cells versus control.

Representative Results

Here we adapted a permeable microporous membrane insert to develop an *in vitro* heterotypic cell co-culture system that mimics the *in vivo* tumor microenvironment (**Figure 1**). This system allows for two different cell populations to be grown on either side of the insert's porous-membrane for extended periods of time (up to 120 hr, in our use). Importantly the system is capable of maintaining the purity of the cell populations, as determined by plating GFP-tagged MDA-MB-231 cells on the top side of 0.4-, 1-, or 3 m-pore inserts and allowing them to grow in co-culture with AG1522 cells growing on the bottom side of the insert, for 120 hr. After this time, the cells were collected from the bottom side of the insert and analyzed by flow cytometry to identify the presence of any GFP-positive MDA-MB-231 cells, which would indicate a loss of cell population purity. Analysis revealed 99.9% and 99.8% pure populations from 0.4 and 1 µm-pore inserts, respectively; however, the insert with 3 µm pores was unable to maintain the separation of the cell populations, as the pores were large enough to allow a significant number of the GFP-positive MDA-MB-231 cells to migrate across the membrane (**Figure 2**).

Importantly, through *in situ* immunofluorescence and Western blot analysis we were able to demonstrate the capability of this system to effectively generate cancer-associated fibroblasts from normal human diploid AG1522 fibroblasts following co-culture with MDA-MB-231 breast cancer cell, as determined by reduced expression of Caveolin-1, a well-established CAF biomarker[39-42] (**Figure 3**). CAV1 is a scaffolding protein that forms the caveolae in the lipid raft domain of the plasma membrane, which is involved in multiple cellular processes[43]. In the Western blot, two distinct bands were observed, corresponding to the α and β isoforms of CAV1[44]. Unfortunately, little is known about the difference(s) between the isoforms, especially their role as CAF biomarkers.

We have also shown the proficiency of the insert co-culture system to modulate intercellular communication between the two heterotypic cell populations (**Figure 4**). Non-labeled, gap-junction competent human diploid AG1522 fibroblasts were cultured to confluency on the bottom side of the insert. A second set of AG1522 cells were loaded with Calcein AM, a green fluorescent gap-junction permeable dye, and plated on the top side of the insert. The two cell populations were allowed to communicate for 6 hr, and then the cells on the bottom side of the insert were isolated and analyzed by flow cytometry. Calcein-positive cells from the bottom side of the insert would be reflective of cells that established gap-junctional coupling through the insert pores. The size of the 0.4 µm pore insert limited functional gap junction formation between cells growing on either side of the insert, thus constraining communication to secreted factors (*e.g.,* growth factors, microvesicles, *etc.*). Alternatively, the size of the 1 µm and 3 µm pores are apparently large enough to allow functional coupling of the cells through gap junctions. Therefore, by modulating the pore size, one can begin to understand the diverse role(s) that different modes of intercellular communication may have on TME development and evolution.

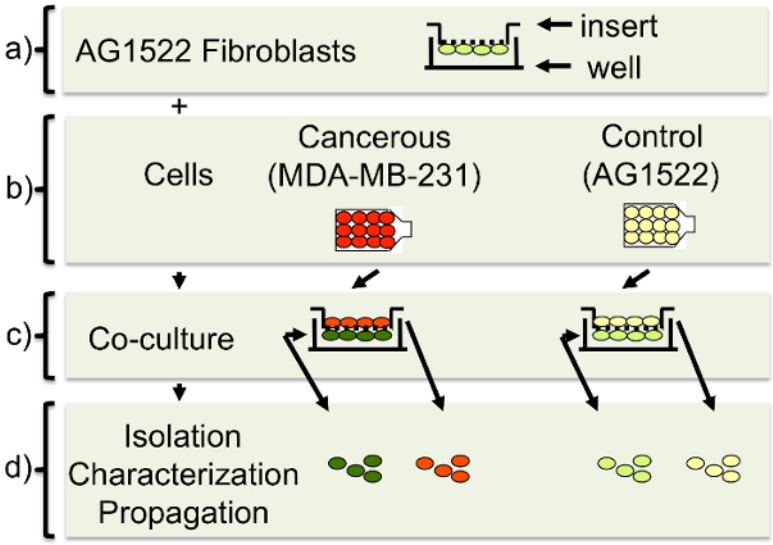

Figure 1: Permeable Microporous Membrane Insert Model Scheme. (**a**) Apparently normal human diploid AG1522 fibroblasts (low passage cells) destined to become CAFs are seeded onto inverted permeable microporous inserts consisting of a 10 µm thick polyester membrane with 0.4 µm, 1 µm, or 3 µm pores. Following attachment, the inserts are inverted and placed into the wells of plates and cultured to confluency. (**b**) Cancer cells and control fibroblasts are grown separately in flasks prior to being seeded on the top side of the inserts with fibroblasts growing intimately on the bottom side. (**c**) The co-cultured cells are fed every other day and maintained for the desired time. (**d**) At the respective times following co-culture and/or experimental treatments, the CAFs (bottom side of the inserts) and/or cancer cells (top side of the insert) are carefully isolated by trypsinization, yielding highly pure cell populations, which can be used for analysis of endpoints or propagated for subsequent studies. Please click here to view a larger version of this figure.

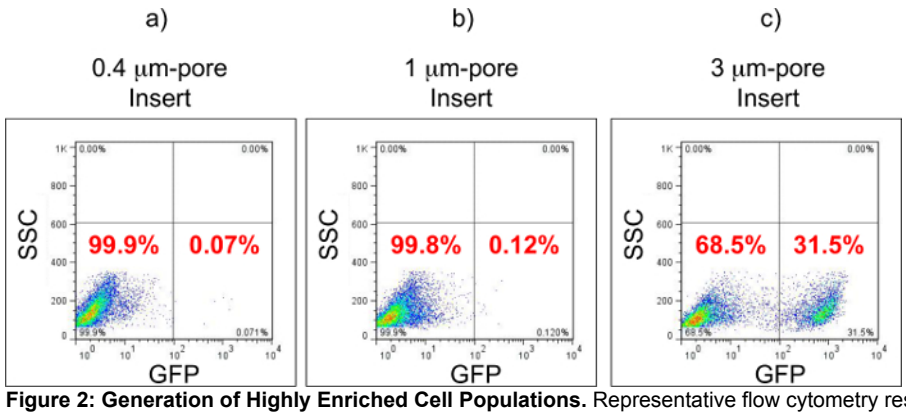

Figure 2: Generation of Highly Enriched Cell Populations. Representative flow cytometry results demonstrate the ability of the insert to maintain highly enriched, yet independent heterotypic cell populations following 120 hr co-culture. (**a**) AG1522 cells harvested from the bottom side of the 0.4 µm pore insert show 99.9% of the population to be free of GFP-labeled MDA-MB-231 cells growing on the top side of the insert (lower left quadrant). (**b**) AG1522 cells harvested from the bottom side of the 1 µm pore insert also show 99.8% enriched population (lower left quadrant). (**c**) AG1522 cells harvested from the bottom side of the 3 µm pore insert reveal that only 68.5% of the population is free of GFP-labeled cells (lower left quadrant), indicating that a large number of GFP-positive MDA-MB-231 cells were able to migrate through the 3 µm pores. Please click here to view a larger version of this figure.

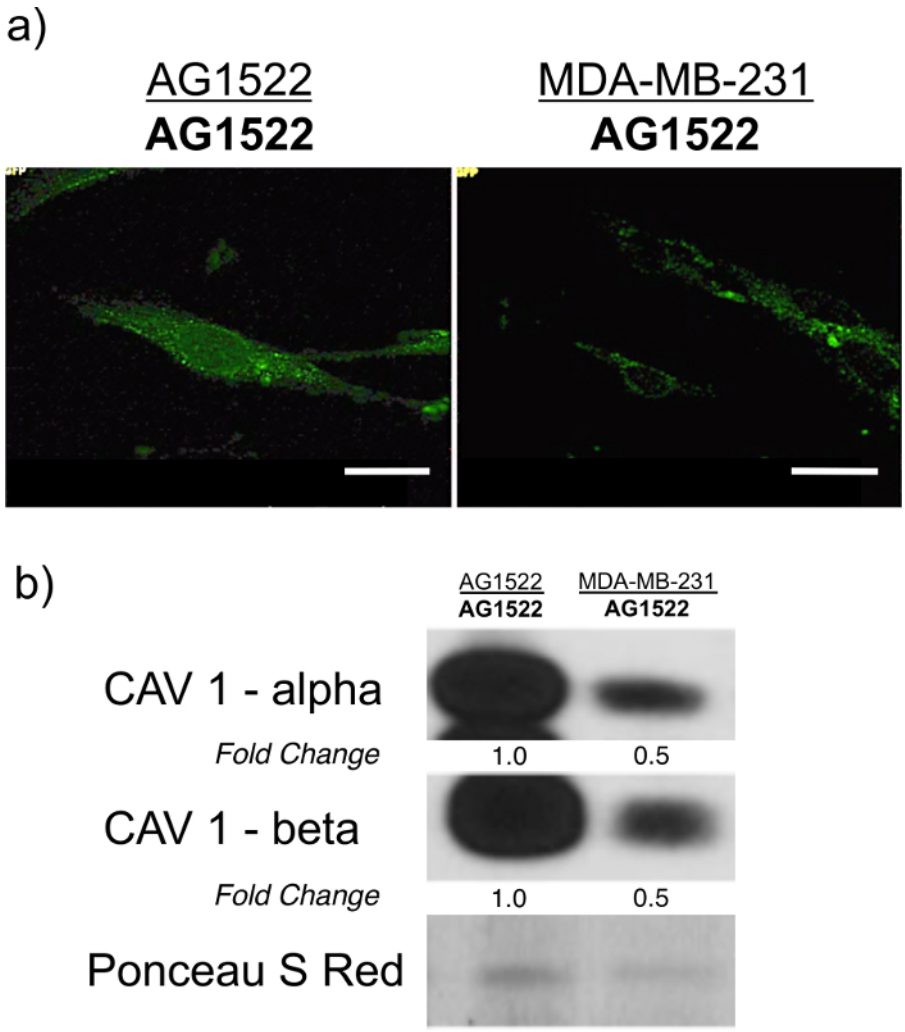

Figure 3: Generation of Cancer-Associated Fibroblasts. Reduced expression of CAV1 is a consistent and reliable CAF biomarker. (**a**) Microscopic images of *in situ* immunofluorescence (scale bar = 20 µm), and (**b**) Western blot analysis of CAV1 in AG1522 cells that had been in co-culture with AG1522 cells (control) (left), or with MDA-MB-231 breast cancer cells (right) for 120 hr. Staining with Ponceau S Red was used for loading control and to determine fold change in Western blots. The results are representative of three separate experiments. Please click here to view a larger version of this figure.

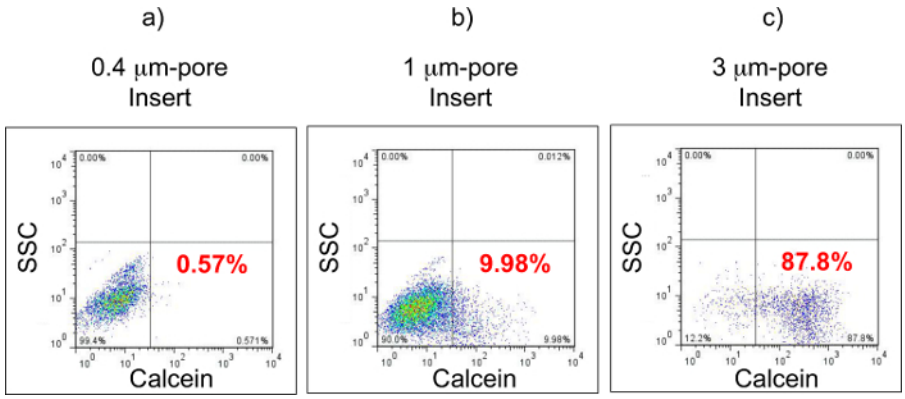

Figure 4: Modulation of Intercellular Communication by Insert Pore-Size. Flow cytometry analyses demonstrating the adaptability of the permeable microporous membrane insert TME model to select for different modes of intercellular communication between Calcein AM loaded AG1522 cells growing on top of the insert and AG1522 control cells growing on its bottom side. (**a**) Cells harvested from the bottom side of 0.4 µm pore inserts show very low levels of Calcein-positive cells (0.57%), indicating limited gap-junction communication through the insert pores. (**b**) Cells harvested from the bottom side of 1 µm pore inserts show higher levels of Calcein-positive cells (9.98%), indicating formation of functional gap junctions. (**c**) Cells harvested from the bottom side of 3 µm pore inserts show high levels of Calcein-positive cells (87.8%), indicating extensive gap-junctional communication. Please click here to view a larger version of this figure.

Discussion

The protocol described here is a simple, adaptable *in vitro* procedure (**Figure 1**) that utilizes a permeable microporous membrane insert to generate highly enriched individual cell populations from a co-culture of heterotypic cells. Significantly, the model is suitable for investigating various modes of intercellular communication. The critical steps include selecting the appropriate pore-size insert for specific experimental interest(s), seeding the first cell population on the bottom side of the insert in medium supplemented with 50% FBS, seeding the second cell population on the top side of the insert, and co-culturing the two distinct cell populations for an appropriate duration of time. We show that this system is capable of mimicking various *in vivo* characteristics, thus providing a greater opportunity to understand the molecular, phenotypic, and latent changes occurring during early TME evolution, which addresses a major disadvantage of many established TME *in vitro* models (**Figure 2**).

The model can be easily modified to permit investigation of various aspects of cell-cell interactions in cancer-stroma development and TME evolution (**Figure 4**). While the 0.4 µm pore insert permits intimate coupling between the two cell populations[45], it significantly restricts formation of functional gap junctions between cells grown on either side of the insert membrane (**Figure 4**). Therefore, thus facilitating investigation of the role of diffusible factors (*e.g.*, growth factors) and/or extracellular vesicles (*e.g.*, exosomes), which mediate CAF development[46-48]. Alternatively, the 1 µm and 3 µm pores are large enough to allow formation of functional gap junctions, thus permitting the study of both direct metabolic coupling via junctional channels and indirect communication through diffusible secreted factors. However, as the 3 µm pore insert permits cell migration through the pores (see **Figure 2**), it does not maintain the purity of two separate heterotypic cell populations during extended co-culture times (*e.g.*, 120 hr). Whereas the present model enables the study of several aspects of the TME, it is limited in its ability to account for many of the complex physiologic interactions that occur within an *in vivo* TME (*e.g.,* vascular fluid exchanges, *etc.*).

Understanding the early events of cancer-stroma activation and development of the TME is important in elucidating the steps implicated in primary tumor initiation and progression, as well as metastasis. It is now widely accepted that the cancer stroma, especially CAFs, possess a critical role in supporting carcinogenesis (reviewed in [49]). This has led to the development of many *in vitro* 2D and 3D models, aimed at illuminating strategies to target the early mechanisms contributing to stromal-activation and tumor progression. Unfortunately, many of these models are limited by their inability to permit isolation of individual cell populations, without time-consuming and stressful processing, for further study. Thus this protocol provides a significant addition to the field of TME research, as it combines *in vivo* like properties with the ability to easily and rapidly obtain highly enriched or pure cell populations for immediate analysis or propagation for subsequent studies.

Once the technique is mastered, the insert TME model can be utilized for investigating diverse TME bi-directional interactions (*e.g.,* cancer to endothelial, cancer to immune cells, *etc.*). Additionally, the complexity of the co-culture can be enhanced by placing a mixed cell population on one side of the insert and a single population on the alternate side, thus obtaining a more *in vivo* like TME cell population complexity. However, caution should be exercised in selecting an insert with the proper pore-size if using cells of especially small diameter (*e.g.*, human lymphocytes with a diameter of ~7 µm[50]), as they may be capable of migrating through the smaller pores (*e.g.*, 0.4 µm or 1 µm). Prior to co-culture, migration experiments (**Figure 2**) may be warranted to ensure maintenance of pure cell populations throughout extended co-culture experiments.

This model is also amenable for investigating the effects of various therapeutic challenges (*e.g.,* ionizing radiation, chemotherapeutics, hyperthermia) and physiological alterations (*e.g.*, hypoxia, hyperoxia, biologic inhibitors) in mixed cell populations that are coupled across the permeable microporous membrane insert. The model has demonstrated its ability to successfully generate CAFs, identified by a widely accepted CAF biomarker (*i.e.,* down-regulation of CAV1)[39-42] (**Figure 3**), which was further reduced by 55% when the insert system was maintained at *in vivo* like PO_2 (7 mm Hg; 0.5% O_2)[51], highlighting the model's adaptability for various experimental designs and conditions (data not shown). In sum, this model provides a simplified approach and an opportunity to modulate temporal and external factors in order to obtain deeper insights into cancer-stroma activation, the early evolution of the TME, and cellular responses to therapeutic or environmental agents.

Disclosures

The authors declare that they have no competing or conflicting interests.

Acknowledgements

This research was supported by grants from the New Jersey Commission on Cancer Research (Pre-Doctoral Fellowship DFHS13PPCO17), the National Institutes of Health (CA049062), and the National Aeronautics and Space Administration (NNX15AD62G).

References

1. Hanahan, D., & Weinberg, R. A. The hallmarks of cancer. *Cell.* **100** (1), 57-70 (2000).
2. Olive, K. P., Jacobetz, M. A., *et al.* Inhibition of Hedgehog signaling enhances delivery of chemotherapy in a mouse model of pancreatic cancer. *Science* **324** (5933), 1457-1461 (2009).
3. Pandol, S., Edderkaoui, M., Gukovsky, I., Lugea, A., & Gukovskaya, A. Desmoplasia of pancreatic ductal adenocarcinoma. *Clinical Gastroenterology and Hepatology: the Official Clinical Practice Journal of the American Gastroenterological Association.* **7** (11 Suppl), S44-7 (2009).
4. Dabbous, M. K., Haney, L., Carter, L. M., Paul, A. K., & Reger, J. Heterogeneity of fibroblast response in host-tumor cell-cell interactions in metastatic tumors. *Journal of Cellular Biochemistry.* **35** (4), 333-344 (1987).
5. Olumi, A. F., Grossfeld, G. D., Hayward, S. W., Carroll, P. R., Tlsty, T. D., & Cunha, G. R. Carcinoma-associated fibroblasts direct tumor progression of initiated human prostatic epithelium. *Cancer Research.* **59** (19), 5002-5011 (1999).

6. Orimo, A., Gupta, P. B., *et al.* Stromal fibroblasts present in invasive human breast carcinomas promote tumor growth and angiogenesis through elevated SDF-1/CXCL12 secretion. *Cell* **121** (3), 335-348 (2005).
7. Schürch, W., Seemayer, T. A., Lagacé, R., & Gabbiani, G. The intermediate filament cytoskeleton of myofibroblasts: an immunofluorescence and ultrastructural study. *Virchows Archiv. A, Pathological Anatomy and Histopathology.* **403** (4), 323-336 (1984).
8. Nakagawa, H., Liyanarachchi, S., *et al.* Role of cancer-associated stromal fibroblasts in metastatic colon cancer to the liver and their expression profiles. *Oncogene* **23** (44), 7366-7377 (2004).
9. Choi, Y. P., Lee, J. H., *et al.* Cancer-associated fibroblast promote transmigration through endothelial brain cells in three-dimensional in vitro models. *International Journal of Cancer. Journal International du Cancer* **135** (9), 2024-2033 (2014).
10. Ito, M., Ishii, G., Nagai, K., Maeda, R., Nakano, Y., & Ochiai, A. Prognostic impact of cancer-associated stromal cells in patients with stage I lung adenocarcinoma. *Chest.* **142** (1), 151-158 (2012).
11. Gaggioli, C., Hooper, S., *et al.* Fibroblast-led collective invasion of carcinoma cells with differing roles for RhoGTPases in leading and following cells. *Nature Cell Biology* **9** (12), 1392-1400 (2007).
12. Navab, R., Strumpf, D., *et al.* Prognostic gene-expression signature of carcinoma-associated fibroblasts in non-small cell lung cancer. *Proceedings of the National Academy of Sciences of the United States of America.* **108** (17), 7160-7165 (2011).
13. Hwang, R. F., Moore, T., *et al.* Cancer-associated stromal fibroblasts promote pancreatic tumor progression. *Cancer Research* **68** (3), 918-926 (2008).
14. Sneddon, J. B., Zhen, H. H., *et al.* Bone morphogenetic protein antagonist gremlin 1 is widely expressed by cancer-associated stromal cells and can promote tumor cell proliferation. *Proceedings of the National Academy of Sciences of the United States of America.* **103** (40), 14842-14847 (2006).
15. De Wever, O., Nguyen, Q.-D., *et al.* Tenascin-C and SF/HGF produced by myofibroblasts in vitro provide convergent pro-invasive signals to human colon cancer cells through RhoA and Rac. *FASEB Journal: Official Publication of the Federation of American Societies for Experimental Biology.* **18** (9), 1016-1018 (2004).
16. Zhang, C., Fu, L., *et al.* Fibroblast growth factor receptor 2-positive fibroblasts provide a suitable microenvironment for tumor development and progression in esophageal carcinoma. *Clinical Cancer Research.* **15** (12), 4017-4027 (2009).
17. Yao, Q., Qu, X., Yang, Q., & Wei, M. CLIC4 mediates TGF-β1-induced fibroblast-to-myofibroblast transdifferentiation in ovarian cancer. *Oncology Reports.* (2009).
18. Crawford, Y., Kasman, I., *et al.* PDGF-C mediates the angiogenic and tumorigenic properties of fibroblasts associated with tumors refractory to anti-VEGF treatment. *Cancer Cell.* **15** (1), 21-34 (2009).
19. Paulsson, J., & Micke, P. Prognostic relevance of cancer-associated fibroblasts in human cancer. *Seminars in Cancer Biology.* **25**, 61-68 (2014).
20. Messina, J. P., & Lawrence, D. A. Effects of 2-mercaptoethanol and buthionine sulfoximine on cystine metabolism by and proliferation of mitogen-stimulated human and mouse lymphocytes. *International Journal of Immunopharmacology.* **14** (7), 1221-1234 (1992).
21. Ames, B. N. Endogenous oxidative DNA damage, aging, and cancer. *Free Radical Research Communications.* **7** (3-6), 121-128 (1989).
22. Cheng, Y., Ma, Z., *et al.* Principles of regulatory information conservation between mouse and human. *Nature.* **515** (7527), 371-375 (2014).
23. Upreti, M., Jamshidi-Parsian, A., *et al.* Tumor-endothelial cell three-dimensional spheroids: new aspects to enhance radiation and drug therapeutics. *Translational Oncology.* **4** (6), 365-376 (2011).
24. Mehta, G., Hsiao, A. Y., Ingram, M., Luker, G. D., & Takayama, S. Opportunities and challenges for use of tumor spheroids as models to test drug delivery and efficacy. *Journal of Controlled Release: Official Journal of the Controlled Release Society.* **164** (2), 192-204 (2012).
25. Muraki, Y., Hongo, S., & Ohara, Y. Contamination of the cell sorter fluidics system with the water-borne bacterium Burkholderia cepacia. *Cytometry. Part A: the Journal of the International Society for Analytical Cytology.* **81** (2), 105-107 (2012).
26. Grobstein, C. Morphogenetic interaction between embryonic mouse tissues separated by a membrane filter. *Nature.* **172** (4384), 869-870 (1953).
27. Tan, S., Tompkins, L. S., & Amieva, M. R. Helicobacter pylori usurps cell polarity to turn the cell surface into a replicative niche. *PLoS Pathogens.* **5** (5), e1000407 (2009).
28. Hyman, T., Shmuel, M., & Altschuler, Y. Actin is required for endocytosis at the apical surface of Madin-Darby canine kidney cells where ARF6 and clathrin regulate the actin cytoskeleton. *Molecular Biology of the Cell.* **17** (1), 427-437 (2006).
29. Ghaffarian, R., & Muro, S. Models and methods to evaluate transport of drug delivery systems across cellular barriers. *Journal of Visualized Experiments : JoVE.* (80), e50638 (2013).
30. Braian, C., Svensson, M., Brighenti, S., Lerm, M., & Parasa, V. R. A 3D human lung tissue model for functional studies on mycobacterium tuberculosis infection. *Journal of Visualized Experiments : JoVE.* (104), e53084 (2015).
31. Bath, M. L. Inhibition of in vitro fertilizing capacity of cryopreserved mouse sperm by factors released by damaged sperm, and stimulation by glutathione. *PLoS ONE.* **5** (2), e9387 (2010).
32. Zhao, Y., De Toledo, S. M., Hu, G., Hei, T. K., & Azzam, E. I. Connexins and cyclooxygenase-2 crosstalk in the expression of radiation-induced bystander effects. *British Journal of Cancer.* **111** (1), 125-131 (2014).
33. Buonanno, M., de Toledo, S. M., & Azzam, E. I. Increased frequency of spontaneous neoplastic transformation in progeny of bystander cells from cultures exposed to densely ionizing radiation. *PLoS ONE.* **6** (6), e21540 (2011).
34. Byers, S. W., Hadley, M. A., Djakiew, D., & Dym, M. Growth and characterization of polarized monolayers of epididymal epithelial cells and Sertoli cells in dual environment culture chambers. *Journal of Andrology.* **7** (1), 59-68 (1986).
35. Pitt, A., & Gabriels, J. Epithelial cell culture on microporous membranes. *American Biotechnology Laboratory.* **4** (5), 38-45 (1986).
36. Buonanno, M., de Toledo, S. M., Pain, D., & Azzam, E. I. Long-term consequences of radiation-induced bystander effects depend on radiation quality and dose and correlate with oxidative stress. *Radiation Research.* **175** (4), 405-415 (2011).
37. Ducrest, A.-L., Amacker, M., Lingner, J., & Nabholz, M. Detection of promoter activity by flow cytometric analysis of GFP reporter expression. *Nucleic Acids Research.* **30** (14), e65 (2002).
38. JoVE Science Education Database. *Basic Methods in Cellular and Molecular Biology.* The Western Blot. JoVE, Cambridge, MA, (2016).
39. Mercier, I., Casimiro, M. C., & Wang, C. Human breast cancer-associated fibroblasts (CAFs) show caveolin-1 down-regulation and RB tumor suppressor functional inactivation: implications for the response to hormonal therapy. *Cancer Biology & Therapy.* (2008).
40. Martinez-Outschoorn, U. E., Pavlides, S., *et al.* Tumor cells induce the cancer associated fibroblast phenotype via caveolin-1 degradation: implications for breast cancer and DCIS therapy with autophagy inhibitors. *Cell Cycle.* **9** (12), 2423-2433 (2010).
41. Witkiewicz, A. K., Dasgupta, A., *et al.* Loss of stromal caveolin-1 expression predicts poor clinical outcome in triple negative and basal-like breast cancers. *Cancer Biology & Therapy.* **10** (2), 135-143 (2014).

42. Zhao, X., He, Y., *et al.* Caveolin-1 expression level in cancer associated fibroblasts predicts outcome in gastric cancer. *PLoS ONE.* **8** (3), e59102 (2013).
43. Shaul, P. W., & Anderson, R. G. Role of plasmalemmal caveolae in signal transduction. *The American Journal of Physiology.* **275** (5 Pt 1), L843-51 (1998).
44. Fujimoto, T., Kogo, H., Nomura, R., & Une, T. Isoforms of caveolin-1 and caveolar structure. *Journal of Cell Science.* **113** (Pt 19), 3509-3517 (2000).
45. Wartiovaara, J., Lehtonen, E., Nordling, S., & Saxen, L. Do Membrane Filters prevent Cell Contacts?*, Nature.* **238** (5364), 407-408 (1972).
46. Tyan, S.-W., Kuo, W.-H., *et al.* Breast cancer cells induce cancer-associated fibroblasts to secrete hepatocyte growth factor to enhance breast tumorigenesis. *PLoS ONE.* **6** (1), e15313 (2011).
47. Xu, J., Lu, Y., Qiu, S., Chen, Z.-N., & Fan, Z. A novel role of EMMPRIN/CD147 in transformation of quiescent fibroblasts to cancer-associated fibroblasts by breast cancer cells. *Cancer Letters.* **335** (2), 380-386 (2013).
48. Hoffman, R. M. Stromal-cell and cancer-cell exosomes leading the metastatic exodus for the promised niche. *Breast Cancer Research : BCR.* **15** (3), 310 (2013).
49. Franco, O. E., Shaw, A. K., Strand, D. W., & Hayward, S. W. Cancer associated fibroblasts in cancer pathogenesis. *Seminars in Cell & Developmental Biology.* **21** (1), 33-39 (2010).
50. Kuse, R., Schuster, S., Schübbe, H., Dix, S., & Hausmann, K. Blood lymphocyte volumes and diameters in patients with chronic lymphocytic leukemia and normal controls. *Blut.* **50** (4), 243-248 (1985).
51. Vaupel, P., Schlenger, K., Knoop, C., & Höckel, M. Oxygenation of human tumors: evaluation of tissue oxygen distribution in breast cancers by computerized O2 tension measurements. *Cancer Research.* **51** (12), 3316-3322 (1991).

